

by Vik and Rugge,¹⁰ who performed an *SPDF* analysis at 310 MeV using data from π^-p elastic scattering, recoil-proton polarization, and charge-exchange scattering. These authors found no solution fitting all their data by starting the search from Foote's Fermi-II solution. Finally, the phenomenological analysis by Roper¹¹ predicts phase shifts at 247 MeV which are very close to those of solution A.

Comparison with theory is made only with the most recent work by Donnachie, Hamilton, and Lea,¹² which is based on dispersion relations for the partial-wave scattering amplitudes. Because of the method of their analysis, their predictions are valid only for $L \geq 1$, but they improve with increasing L . The results of these

calculations are

$$\begin{array}{ccccc} P_{3,1} & D_{3,3} & D_{3,5} & F_{3,5} & F_{3,7} \\ -9.2 \pm 0.8 & -0.5 \pm 0.2 & -1.3 \pm 0.1 & -0.04 \pm 0.04 & 0.34 \pm 0.05. \end{array}$$

Solution A fits these predictions best.

To summarize, while only one acceptable *SPDF* solution was found, no claim can be made that the polarization and differential-cross-section data alone, no matter how accurately measured, are capable of establishing the small phase shifts accurately. A proposal¹³ has been advanced to measure the spin rotation coefficients, since they are capable of sensitive discrimination against the Fermi-II solution. However, technical difficulties will delay the measurement of these parameters for some time. Therefore, π^-p scattering that involves both the isotopic-spin $T = \frac{3}{2}$ and $T = \frac{1}{2}$ states will in the near future remain the only source of accurate phase-shift analyses in the pion-nucleon system.

¹³ Y. S. Kim, Phys. Rev. **129**, 862 (1963).

¹⁰ H. R. Rugge and O. T. Vik, Phys. Rev. **129**, 2300 (1963); O. T. Vik and H. Rugge, *ibid.* **129**, 2311 (1963).

¹¹ L. D. Roper, Phys. Rev. Letters **12**, 340 (1964).

¹² A. Donnachie, J. Hamilton, and A. T. Lea, Phys. Rev. **135**, B515 (1964).

Peripheral Production and Decay Parameters of $N^{*++}(1238)$ in $pp \rightarrow nN^{*++}(1238)$ at 5.5 GeV/c

G. ALEXANDER, B. HABER, A. SHAPIRA, AND G. YEKUTIELI
Nuclear Physics Department, Weizmann Institute, Rehovoth, Israel

AND

E. GOTSMAN

Israel Atomic Energy Commission, Soreq Nuclear Research Center, Yavneh, Israel
(Received 10 November 1965)

Experimental differential cross sections and $N^*(1238)$ decay parameters for the reaction $pp \rightarrow nN^{*++}(1238)$ at 5.5 GeV/c are presented. The differential cross sections are well described by an absorptive one-pion-exchange model with equal pp and $nN^*(1238)$ elastic cross sections. A better agreement is achieved using a steeper nN^* differential cross section than that for the pp one, or with a sharp cutoff model corresponding to an absorption radius of about 0.9–1.0 F. The $N^*(1238)$ decay parameters are also found to be in good agreement with the absorption model.

1. INTRODUCTION

IN this paper we present experimental results on the production and decay of the $N^{*++}(1238)$ resonance in the reaction $pp \rightarrow nN^{*++}(1238) \rightarrow n\pi\pi^+$ at 5.5 GeV/c and analyze it according to the absorption model.¹

The absorption model is a modification of the peripheral or one-pion-exchange (OPE) model and it is applied mainly to quasi-two-particle reactions. As in the OPE model, the inelastic reactions are described by the Born term of the one-pion exchange. However,

¹ See, for instance, N. J. Sopkovich, Nuovo Cimento **26**, 186 (1962); A. Dar, M. Kugler, Y. Dothan, and S. Nussinov, Phys. Rev. Letters **12**, 82 (1964); K. Gottfried and J. D. Jackson, Nuovo Cimento **34**, 735 (1964); L. Durand and Y. T. Chiu, Phys. Rev. **137**, B1530 (1965) and references given therein.

the absorption model takes into account effects arising from competing inelastic processes, and modifies each partial wave of the Born term by absorption factors. In a quasi-two-particle reaction the absorption factors are evaluated from the elastic scattering of the incoming and outgoing particles.

Assuming one pion exchange, and equal nN^* and pp elastic scattering, the $pp \rightarrow nN^{*++}(1238)$ reaction is completely described by the absorption model. With the help of the $p\pi n$ and $p\pi N^*$ coupling constants, and explicit wave functions of the $\frac{3}{2}^+N^*(1238)$ resonance,² the OPE Born term and its partial-wave expansion were calculated. The absorption factors were evaluated from pp elastic scattering at 5.5 GeV/c.

² Y. Frishman and E. Gotsman, Phys. Rev. **140**, B1151 (1965).

Using the partial-wave expansion of the OPE amplitude, we were able to study two more versions of the absorption model. In the first version the unknown $nN^*(1238)$ elastic scattering is assumed to be different from that of pp , and the nN^* absorption factor is estimated by comparing the theoretical predictions with the experimental observations. In the second version, the sharp-cutoff model, all partial waves with total angular momentum $J < J_c$ are eliminated from the OPE amplitude. The cutoff angular momentum is found by best fit between theory and experiment.

In Sec. 2 we describe studies of the quasi-two-particle reaction $pp \rightarrow nN^{*++}(1238) \rightarrow n p \pi^+$ in a hydrogen bubble chamber at 5.5 GeV/c. In Sec. 3 the absorption model is used to calculate the differential cross section of this reaction, and the predictions are compared with the experimental results. In Sec. 4 the density matrix of $N^{*++}(1238)$ is evaluated and the angular distributions of its decay products are compared with experimental observation.

2. EXPERIMENTAL RESULTS

A total of 3550 two-prong events were measured, using pictures taken with the Saclay 81 cm hydrogen bubble chamber exposed to a 5.5-GeV/c proton beam at CERN.³ The measured events were fitted to the following reactions:

$$pp \rightarrow pp \text{ (elastic scattering)} \quad (1)$$

$$pp \rightarrow n p \pi^+, \quad (2)$$

$$pp \rightarrow p p \pi^0. \quad (3)$$

Out of this sample, 831 events yielded an unambiguous unique fit to reaction (2). Another 25 events fitted reaction (2) only, but also fitted the reaction with the proton and the π^+ interchanged. A further 75 events gave good fits to both reactions (2) and (3), and 5 events gave good fits to reactions (1) and (2). The following analysis is based on the 831 events which gave unambiguous unique fits to reaction (2).

The $p\pi^+$ effective-mass distribution of this sample is given in Fig. 1. A high peak is seen at the $N^*(1238)$ mass value, and two less pronounced peaks at the $N^*(1920)$ and $N^*(2360)$ mass values, respectively.

The percentages of these three resonances in the reaction $pp \rightarrow nN^{*++}(N^{*++} \rightarrow p\pi^+)$ were found by a least-squares fit between (on the one hand) the observed $p\pi^+$ mass distribution and (on the other hand) a linear combination of three Breit-Wigner distributions representing the three resonances, and a phase-space distribution. The mass values and the full widths used for the three resonances are, in GeV: 1.238 and 0.125, 1.920 and 0.170, and 2.360 and 0.200, respectively. The full line on Fig. 1 is the best fitted curve of

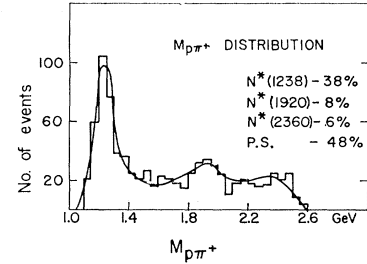


FIG. 1. $p\pi^+$ effective mass distribution for $pp \rightarrow n p \pi^+$. The full line represents the best fit to phase space plus $N^*(1238)$, $N^*(1920)$, and $N^*(2360)$.

the three resonances with the following percentages: 38% $N^*(1238)$; 8% $N^*(1920)$; and 6% $N^*(2360)$.

For further analysis, 231 events with a $p\pi^+$ invariant mass between 1.17 and 1.30 GeV were chosen to represent events of the type:

$$pp \rightarrow nN^{*++}(1238) \text{ and } N^{*++}(1238) \rightarrow p\pi^+. \quad (4)$$

The background contamination for this selected sample was estimated to be about 10%.

A further 218 events yielded an unambiguous unique fit to reaction (3). About 20% of these events were of the type $pp \rightarrow pN^{*++}(1238)$ ($N^{*++}(1238) \rightarrow p\pi^0$), but with an appreciable background contamination. As it is very important for our analysis to get a clean sample of $pp \rightarrow nN^*$ events, only the $pp \rightarrow nN^{*++}$ events were used.

The c.m. system angular distribution of reaction (4) is symmetric around 90° and shows a forward-backward peaking. A forward-backward symmetry in the c.m. system is expected because of the identity of the two protons in the initial state. For this reason we cannot distinguish between forward and backward scattering, and the folded differential cross section was compared with the calculated one. The differential cross sections, folded around 90° , are given in Fig. 2.

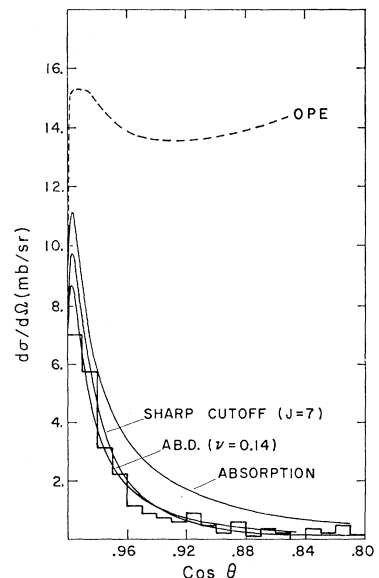


FIG. 2. Differential cross sections for the reaction $pp \rightarrow nN^{*++}$. The curves correspond to cross sections calculated with the unmodified OPE model (dashed curve) and with modified OPE models for different forms of absorption (full curves).

³ For further details on this exposure see G. Alexander, O. Benary, N. Kidron, A. Shapira, R. Yaari, and G. Yekutieli, Phys. Rev. Letters 13, 355 (1964).

The strong forward-backward peaking is consistent with N^* formation in small-momentum-transfer pp reactions in accordance with OPE models.

3. COMPARISON WITH THE ABSORPTION MODEL

The scattering amplitude of reaction (4) according to the absorption model is given in the helicity representation by⁴:

$$\begin{aligned} M_{\lambda N^*, \lambda n, \lambda p, \lambda p'}^{\text{abs}} &= (S_{nN^*})^{1/2} B_{\lambda N^*, \lambda n, \lambda p, \lambda p'} (S_{pp'})^{1/2} \\ &= \sum_J (2J+1) (S_{nN^*})^{1/2} B_{\lambda N^*, \lambda n, \lambda p, \lambda p'}^J \\ &\quad \times (S_{pp'}^J)^{1/2} d_{\lambda\mu}^J(\cos\theta), \end{aligned} \quad (5)$$

where $S_{pp'}$ and S_{nN^*} are the elastic scattering amplitudes of pp and nN^* , respectively; λp , $\lambda p'$, λN^* , and λn are the helicities of the incoming and outgoing particles; $\lambda = \lambda_p - \lambda_{p'}$; and $\mu = \lambda_{N^*} - \lambda_n$. The $d_{\lambda\mu}^J(\cos\theta)$ are the rotation functions. The explicit OPE Born term, $B_{\lambda N^*, \lambda n, \lambda p, \lambda p'}$, for reaction (4) is

$$B_{\lambda N^*, \lambda n, \lambda p, \lambda p'} = \frac{iG_{pn\pi} + G_{pN^*} \pi^+}{m_\pi (m_\pi^2 - t)} \bar{U}^{\lambda n} \gamma_5 U^{\lambda p'} \psi_\mu^{\lambda N^*} q_\mu U^{\lambda p}, \quad (6)$$

where the U 's are the nucleon spinors, ψ_μ is the wave function of a spin- $\frac{3}{2}^+ N^*(1238)$ resonance, m_π and q_μ are the mass and four-momentum of the exchanged pion, and $t = q_\mu q_\mu$.

Explicit helicity functions for a spin- $\frac{3}{2}$ particle² were used to evaluate the OPE amplitude. The coupling constant values in this case are⁵: the well-known $G_{pn\pi} + 2/4\pi = 29.0$; and $G_{pN^*} + 2/4\pi = 0.38$, which is derived from the decay rate of $N^{*++}(1238) \rightarrow p\pi^+$.

The OPE amplitude in the helicity representation (6) can also be written in the form⁶:

$$\begin{aligned} B_{\lambda\mu}(s, x) &= \left(\frac{1-x}{2}\right)^{|\lambda-\mu|/2} \left(\frac{1+x}{2}\right)^{|\lambda+\mu|/2} \\ &\quad \times \left| \frac{A_{\lambda\mu}(s, z)}{z-x} + P_{\lambda\mu}(s, x) \right|, \end{aligned} \quad (7)$$

where $x = \cos\theta$ in the c.m. system, $z = 1 + (m_\pi^2 - t_1)/2qq'$, and t_1 is the momentum transfer squared for $x=1$, q and q' are the c.m. momenta in the incoming and outgoing channels, and $p_{\lambda\mu}(s, x)$ is a polynomial in x . For reaction (4), $p_{\lambda\mu}$ is at most of the second degree in x .

This form of the OPE amplitude can be expanded as

$$B_{\lambda\mu}(s, x) = \sum_{J=J'}^{\infty} (2J+1) B_{\lambda\mu}^J d_{\lambda\mu}^J(x), \quad (8)$$

where

$$\begin{aligned} B_{\lambda\mu}^J &= A_{\lambda\mu}(s, z) C_{\lambda\mu}^J(z) + R_{\lambda\mu}^J(s), \\ C_{\lambda\mu}^J &= \frac{1}{2} \int_{-1}^1 \left(\frac{1-x}{2}\right)^{|\lambda-\mu|/2} \left(\frac{1+x}{2}\right)^{|\lambda+\mu|/2} d_{\lambda\mu}^J(x) \frac{dx}{z-x}, \end{aligned}$$

⁴ M. Jacob and G. C. Wick, Ann. Phys. (N. Y.) **7**, 404 (1959); N. J. Sopkovich, Nuovo Cimento **26**, 186 (1962).

⁵ J. D. Jackson and H. Pilkuhn, Nuovo Cimento **33**, 906 (1964).

⁶ L. Durand and Y. T. Chiu, Phys. Rev. **137**, B1530 (1965).

and $J' = \max(|\lambda|, |\mu|)$. The function $R_{\lambda\mu}^J(s)$ is the transform of the polynomial $P_{\lambda\mu}^J(s, x)$ in (7). In our case $P_{\lambda\mu}^J(x)$ is different from zero only for $J \leq 2$.

The scattering amplitude S_{pp} in (5) can be evaluated from pp elastic-scattering measurements with the assumption that S_{pp} is real (diffraction scattering). In this case the partial waves and the differential elastic cross sections are

$$S_{pp}^J = 1 - (\nu^2 \sigma_{\text{tot}} / 2\pi) \exp[-(J\nu/q)^2], \quad (9)$$

and

$$d\sigma/dt = (\sigma_{\text{tot}}^2 / 16\pi) \exp[-(t/2)\nu^2]. \quad (10)$$

The pp elastic-differential cross section was measured at 5.5 GeV/c.⁷ The experimental results gave a good fit to (10) with $\nu = 0.24$ GeV (for $0.07 < t < 0.20$ GeV²) and $\sigma_{\text{tot}} \cong 2\pi/\nu^2$.

Since the $nN^*(1238)$ elastic-scattering amplitude is unknown, we tentatively assume $S_{nN^*}^J = S_{pp}^J$, and the amplitude for reaction (4) will be written with the help of (5), (8), and (9) as

$$\begin{aligned} M_{\lambda\mu}^{\text{abs}} &= A_{\lambda\mu}(s, z) \sum_{J=J'}^{\infty} (2J+1) (1 - e^{-(J\nu/q)^2})^{1/2} \\ &\quad \times C_{\lambda\mu}^J(z) (1 - e^{-(J\nu'/q')^2})^{1/2} d_{\lambda\mu}^J(x), \end{aligned} \quad (11)$$

where $J' = \max(|\lambda|, |\mu|)$ and $\nu' = \nu = 0.24$ GeV. Since the contribution of $R_{\lambda\mu}^J(s)$ is only for $J \leq 2$, it will be neglected.

The differential cross section calculated according to (11) is shown in Fig. 2; it has the right shape, but is somewhat higher in the forward direction than the observed one. Better agreement can be obtained by using a different absorption parameter ν' for the unknown nN^* scattering from that for the pp scattering.

Differential cross sections were calculated with the help of (11) for $\nu = 0.24$ and $\nu' = 0.04, 0.08, 0.12, 0.16, 0.24$, and 0.32 . The results for this version of the model (A.B.D.) are plotted on Fig. 3. Best agreement with experimental results is obtained for $\nu' = 0.14$ (see curve A.B.D. on Fig. 2).

Another version of the absorption model that was studied is the sharp-cutoff model (S.C.O.). In this model it is assumed that the absorption processes completely suppress the OPE amplitude at low angular momentum ($J < J_c$) and do not affect the partial waves at higher values of J . The sharp-cut amplitude for reaction (4) will be

$$M_{\lambda\mu}^{\text{SC}}(s, x) = A_{\lambda\mu}(s, z) \sum_{J=J_c}^{\infty} (2J+1) C_{\lambda\mu}^J(z) d_{\lambda\mu}^J(x). \quad (12)$$

This version of the absorption model has a free parameter J_c that can be found by comparing the predicted differential cross section based on (12) with the observed one. The results of the calculation with the help of (12) for several values of $J_c (= 2, 4, 6, 8, 10)$ are shown on Fig. 4.

⁷ G. Alexander, B. Haber, A. Shapira, G. Yekutieli, and E. Gotsman (to be published).

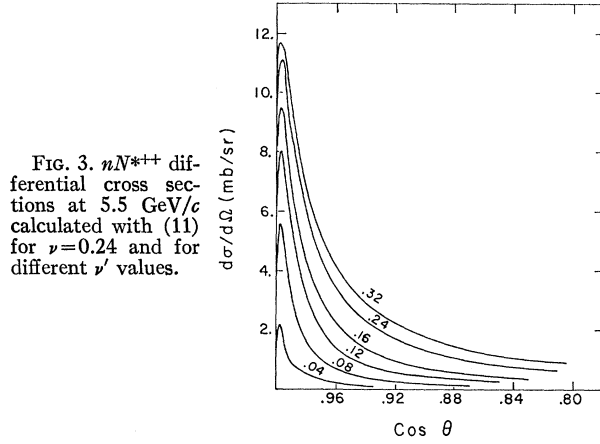


FIG. 3. nN^{*++} differential cross sections at 5.5 GeV/c calculated with (11) for $\nu=0.24$ and for different ν' values.

Good agreement with the experimental differential cross section is obtained for $J=7$ or 8 (see Fig. 2). These values of the total angular momentum correspond to an impact parameter of $b=0.9-1.0$ F.

The differential cross section with the unmodified Born amplitude (6) is also plotted on Fig. 2 (dashed line) and it is very different in both shape and value from the observed cross section.

4. $N^*(1238) \rightarrow p\pi^+$ DECAY

The absorption model predicts also the angular distribution of the $N^*(1238)$ decay products in reaction (4). A reference frame in which the z axis is parallel to the direction of the incoming particle in the N^* c.m. system, the y axis is perpendicular to the production plane, and the x axis is perpendicular to the y - z plane is often used. In this frame of reference the angular distribution of the proton from the $N^*(1238)$ decay is given by⁸

$$W(\cos\theta, \phi) = \frac{3}{4\pi} \{ \rho_{3,3} \sin^2\theta + \rho_{1,1} (\frac{1}{3} + \cos^2\theta) - \frac{2}{3}\sqrt{3} (\text{Re}\rho_{3,-1} \sin^2\theta \cos 2\phi + \text{Re}\rho_{3,1} \sin 2\theta \cos\phi) \}, \quad (13)$$

$$W(\cos\theta) = \int W(\theta, \phi) d\phi = -\frac{1}{4} + (3\rho_{11} - \frac{3}{4}) \cos^2\theta, \quad (13a)$$

$$W(\phi) = \int W(\theta, \phi) d\cos\theta = \frac{1 - (4/\sqrt{3}) \text{Re}\rho_{3,-1} \cos 2\phi}{2\pi}, \quad (13b)$$

where θ is the angle between the decay proton and the z axis, and ϕ is the azimuthal angle in the x - y plane.

The $\rho_{mm'}$ are the density matrix elements and are given by

$$\rho_{mm'} = N \sum_{l, \mu, \lambda} \langle m, l | M | \mu, \lambda \rangle \langle m', l | M | \mu, \lambda \rangle, \quad (14)$$

where N is a normalization factor and $\langle m, l | M | \mu, \lambda \rangle$ are

⁸ K. Gottfried and J. D. Jackson, Nuovo Cimento 33, 309 (1964).

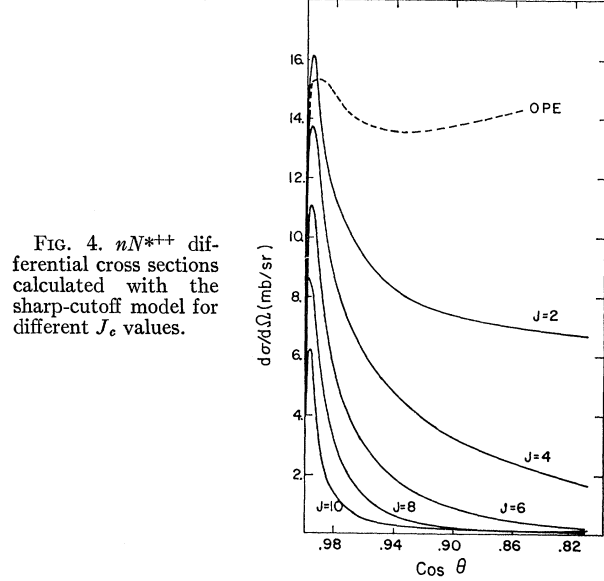


FIG. 4. nN^{*++} differential cross sections calculated with the sharp-cutoff model for different J_e values.

the matrix elements for reaction (4). The relation $\rho_{11} + \rho_{33} = 0.5$ can be derived from the normalization and symmetry properties of the density matrix. For the unmodified one-pion-exchange model, $\rho_{11} = 0.5$ and all other decay parameters in (13) are equal to zero.

With absorption modifications the $\rho_{3,3}$, $\rho_{3,1}$, and $\rho_{3,-1}$ elements of the density matrix are functions of the isobar production angle θ , and they could be different from zero. Average experimental values were found by maximum-likelihood fit between (13) and the experimental $W(\cos\theta, \phi)$ distribution of the entire $N^*(1238)$ sample. These values are compared in Table I with the predictions of the various versions of the absorption model. A similar comparison between theory and experiment for particular $N^*(1238)$ angles θ_p is shown on Fig. 5.

The experimental $\rho_{3,3}$ value is different from zero and is in good agreement with the predictions of the absorption model. The other two values, $\rho_{3,1}$ and $\rho_{3,-1}$, agree within experimental errors with the predictions of both the OPE and the absorption models. The observed angular distributions $W(\cos\theta)$ and $W(\phi)$ are shown in Figs. 6(a) and 6(b) together with the expected curves calculated from 13(a) and 13(b) using the experimental ρ_{11} and $\rho_{3,-1}$ values. In the same figure are also plotted the corresponding distributions for a non-

TABLE I. Comparison between the decay parameters of $W(\cos\theta, \phi)$ for the entire sample, as found by best fit with experimental results, and the values calculated with the absorption models (ABS., AB.D., and S.C.O.).

	$\bar{\rho}_{33}$	$\bar{\rho}_{3,1}$	$\bar{\rho}_{3,-1}$
Experimental best fit	0.13 ± 0.04	0.02 ± 0.04	-0.03 ± 0.04
O. P. E.	0.0	0.0	0.0
ABS.; $\nu = \nu' = 0.24$	0.12	0.06	0.03
AB. D.; $\nu = 0.24$, $\nu' = 0.14$	0.12	0.03	0.05
S.C. O.; $J_e = 7$	0.13	0.02	0.04

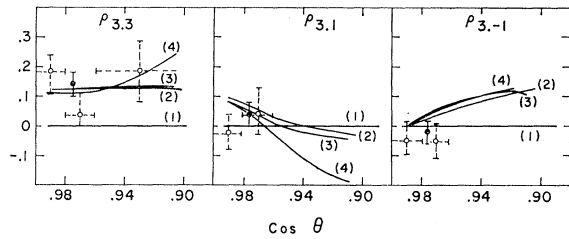


FIG. 5. Experimental values of the ρ parameters for the total sample (filled circle) and for different $\cos\theta$ intervals (open circles). The curves correspond to calculated ρ values using the different models (1—OPE, 2—ABS., 3—AB.D., 4—S.C.O.).

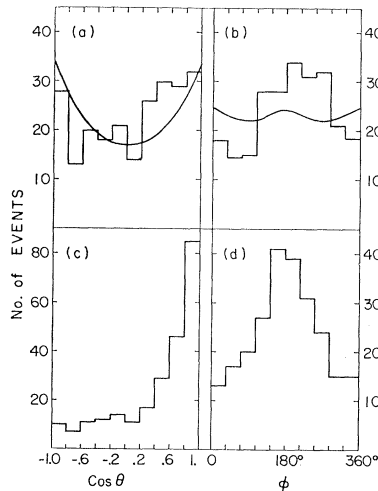


FIG. 6. $W(\cos\theta)$ and $W(\phi)$ distributions of the decay proton in the N^* c.m.system. (a), (b) correspond to events with $1170 \text{ MeV} < M_{p\pi^+} < 1300 \text{ MeV}$, and (c), (d) to events with $1300 \text{ MeV} < M_{p\pi^+} < 1800 \text{ MeV}$.

resonance-events sample ($1.3 \text{ GeV} < M_{p\pi^+} < 1.8 \text{ GeV}$). The distributions for the nonresonance events [Figs. 6(c) and 6(d)] are completely different from the resonance-events distributions and from the theoretical distributions (13a) and (13b).

5. CONCLUSIONS

The absorption model using a one-pion-exchange mechanism and absorption factors for the incoming and outgoing channels evaluated from pp elastic scattering describes adequately the production and decay of $N^*(1238)$ in the reaction $pp \rightarrow nN^* \rightarrow np\pi^+$ at $5.5 \text{ GeV}/c$.

Better agreement is obtained if one introduces a different elastic-scattering behavior for the nN^* from that of the pp . In this way one may learn about the nN^* interaction from the peripheral interaction $pp \rightarrow nN^*$. The differential nN^* cross section found in this way seems to be appreciably steeper than that of the pp , namely $(d\sigma/dt)_{nN^*} \approx e^{-2.8t}$ as compared with $(d\sigma/dt)_{pp} \approx e^{-8.7t}$.

Very good agreement is obtained for the simple cutoff model with $7 \leq J_c \leq 8$, corresponding to an absorption radius of $0.9\text{--}1.0 \text{ F}$.

ACKNOWLEDGMENTS

We would like to thank CERN and the hydrogen bubble chamber crew for enabling us to have the pp exposure.

Pair Production by 5-GeV Photons in Carbon*

J. K. WALKER AND M. WONG†

Harvard University, Cambridge, Massachusetts

AND

R. FESSEL, R. LITTLE, AND H. WINICK

Cambridge Electron Accelerator, Cambridge, Massachusetts

(Received 29 November 1965)

The production of wide-angle electron pairs by high-energy photons in the field of the carbon atom has recently been studied at the Cambridge Electron Accelerator. An apparent systematic deviation from the predictions of quantum electrodynamics was observed. In this situation we thought it worthwhile to recheck the total cross section for photon absorption at high energies and reanalyze previous experimental results. Theoretical cross sections were also calculated in detail and comparison of the experimental data was made with several atomic screening calculations. We find that within about 2%, which is the present experimental and theoretical uncertainty, there is reasonable agreement between experiment and theory.

1. INTRODUCTION

WIDE-angle electron pair production has recently been studied at the Cambridge Electron Accelerator by Blumenthal *et al.*¹ Their results were not in

* This work supported by the U. S. Atomic Energy Commission.
† Frank Knox Memorial Fellow.

¹ R. B. Blumenthal, D. C. Ehn, W. L. Faissler, P. M. Joseph, L. J. Lanzerotti, F. M. Pipkin, and D. G. Stairs, Phys. Rev. Letters **14**, 660 (1965). (A particular motivation for the present

agreement with the predictions of quantum electrodynamics. In particular, the observed deviation did not seem to depend on the angle of production of the pairs

experiment was the poor agreement reported by the above authors for the singles rate of electrons detected at several degrees. That part of the singles rate which depended on the square of the target thickness should be dominated by pair production in the forward direction and subsequent scattering out of one particle of the pair. Therefore, a discrepancy of the singles rate could have been due to anomalous production of pairs at small angles.)